

A Feasibility Study of Spectral Color Reproduction

Francisco H. Imai,^{▲*} David R. Wyble, and Roy S. Berns[▲]

Munsell Color Science Laboratory, RIT, Rochester, New York, USA

Di-Yuan Tzeng

Hewlett-Packard, Boise, Idaho, USA

Efforts to construct end-to-end color reproduction systems based on the preservation of scene spectral data are ongoing at the Munsell Color Science Laboratory. The goal of this end-to-end color-reproduction research was the examination of the possibilities and limitations of commercial input and output devices. The goal of the particular research reported in this article is to produce hardcopy results that are spectrally matched to original colors. The approach described consisted of scene capture using a trichromatic digital camera combined with multiple filtration, image processing, and four color ink jet printing. Both scene input and printed output were defined spectrally. The spectral-based printing separation algorithm produced the least metameric reproduction compared to the original scene using a computationally feasible approach. Results showed an average end-to-end system accuracy of 1.5 ΔE_{00} and spectral reflectance rms error of 0.9% between measured and reproduced reflectances for a printed target of 55 colors.

Journal of Imaging Science and Technology 47: 543–553 (2003)

Introduction

Current graphic arts reproduction techniques of image capture, scanning, proofing, and printing are still heavily entrenched in the traditions of densitometry and crafts experience. Color management systems, which rely on colorimetry, find limited use. The European MARC project demonstrated the feasibility of an end-to-end scene to hardcopy colorimetric color management system for artwork reproduction.¹ This project was very successful in producing high quality reproductions that matched the original paintings under controlled illumination. Another example is the textbook by Billmeyer and Saltzman, *Principles of Color Technology*, 3rd edition, that used the ICC color management framework to reproduce color-order systems and colorimetrically relevant digital images.² These approaches can be used to produce pleasant hardcopy, or an accurate hardcopy under a controlled environment; for critical color matching applications such as catalog sales and art books these techniques can often lead to color reproductions which lack sufficient color quality. Multi-channel visible spectrum imaging (MVSI), also known more commonly as *spectral imaging*, offers better accuracy at the expense of more system complexity and higher system

bandwidth demands.^{3–6} Spectral imaging performs a finer sampling in the wavelength domain during the capture and its techniques allow the estimation of the spectral reflectance properties of the scene, and therefore, these types of imaging can minimize metamerism.

A variety of camera approaches are available for MVSI systems.^{7–16} The Munsell Color Science Laboratory (MCSL) has concentrated in two different general approaches. The first is a narrow band approach.^{7–10,14} Results have been reported on the use of placing a narrow bandpass tunable filters in front of a monochrome sensor.^{9,10,14} Both CCD^{6–9,14} and panchromatic, black-and-white film¹⁰ have been utilized as sensors for narrow bandpass capture. These systems are analogous to using a spectrophotometer, sampling the visible spectrum at known bandpass and wavelength interval. The second approach uses a conventional trichromatic digital camera combined with absorption filters or different light sources.^{12,13} In this broad band approach, the spectral reflectance of each pixel of the original scene can be estimated using *a priori* spectral analysis with direct spectrophotometric measurement and imaging of samples of the object to establish a relationship between the camera signals and spectral reflectance. Alternatively, it is possible to use five to six optimized wide band filters for image capture.^{4,14,15} The wide band acquisition takes advantage of the possibility of decreasing the spectral sampling increment without a significant loss of spectral information because of the smooth absorption characteristics of both synthetic and natural colorants within the visible spectrum.^{17–20}

The image processing stage of a spectral-based color reproduction system involves the spectral reflectance estimation using the captured multi-channel data fol-

Original manuscript received April 2, 2003

▲ IS&T Member

Color Plate 17 is printed in the color plate section of this issue, pp. 586–603.

* Current address: Pixim, Inc. Mountain View, CA 94043, USA

©2003, IS&T—The Society for Imaging Science and Technology

lowed by transformation to signals appropriate for the output device. In cases where the mathematics required to estimate reflectance from captured scene information are purely linear,²¹ the processing to estimate spectral reflectance is computationally fast even for high resolution images. With the addition of a printing system, however, the image processing can be extremely complex and computationally slow.²²

In contrast to the abundance of research concerning image capture aspects of spectral imaging, there has been much less research on the spectral color reproduction of hardcopy.^{10,22-34} At MCSL, an algorithm was developed by Tzeng comprising several steps.²⁴ At first, *a priori* analysis was performed to determine an optimal ink set.²⁶ In this analysis, the spectral properties of the colorants used to create the original object were measured or estimated and analyzed statistically. The possible statistical colorants were correlated to real inks in an existing database resulting in an optimal ink set.²⁷ A printer overprint model was next derived.²⁸ The spectral reflectance of the ink overprints were predicted using Kubelka–Munk theory.²⁹ The Yule–Nielsen modified Neugebauer equations were used to predict spectral reflectance from dot areas.²⁹ More details on the use of this model for developing printer profiles are given by Iino and Berns.^{30,31} Using this approach, Tzeng was successful in reproducing the colors of the GretagMacbeth ColorChecker™ color rendition chart using the Dupont WaterProof™ proofing process with six inks.²⁴ The average color difference between the original rendition chart and the reproduction for illuminant D50 and the 2° observer was $1.9 \Delta E^*_{94}$ with maximum of 5.8. The research by Tzeng was fundamental and not focused on the high-speed requirements to create color separations for high resolution images. Essentially, Tzeng used images with limited number of pixels (corresponding to the various target colors such as the ColorChecker). Extending his research to images with millions of pixels has been a research topic at MCSL.^{22,23,33,34} In one earlier study, an end-to-end spectral reproduction from scene to hardcopy was obtained using as input, a liquid crystal tunable filter (LCTF) attached to a camera loaded with negative film and as output, six color MatchPrint™ proofing.¹⁰

We extended the spectral-based ink separation research from proofing to ink jet printing using initially a four color ink jet printer. We also have been working with a six color ink jet printer.^{22,34} This publication describes spectral color reproduction from scene to hardcopy using a trichromatic digital camera and a four color inkjet printer, in order to verify the feasibility and accuracy of spectral imaging and reproduction using systems that do not require fabrication especially for this purpose.

For this feasibility study, we have developed an end-to-end spectral color reproduction system comprising a spectral image acquisition system and a spectral-based printing system. A scene was captured using broadband multi-channel imaging of the visible spectrum. The spectral reflectance of each pixel was estimated from the digital signals. The spectral reflectance image was processed by a spectral-based color separation algorithm, and prints produced.

Spectral Color Reproduction System

Figure 1 shows a block diagram of the experimental pipeline and performance analyses.

A CMYK test target was printed and was used to evaluate the spectral image acquisition and spectral-based printing systems. The spectral reflectances, rep-

resented by matrix \mathbf{R} , also called original reflectances in the diagram because they correspond to the original printed target, were measured by spectrophotometry. The spectral reflectance measurement for each color corresponds to the column of matrix \mathbf{R} . Eigenvector analysis was performed on the reflectances in order to provide dimensionality reduction. A set of eigenvectors was selected in order to reconstruct the original reflectances with sufficient accuracy, shown in Eq. (1).

$$\hat{\mathbf{R}}_E = \mathbf{E}\mathbf{A} \quad (1)$$

where $\hat{\mathbf{R}}_E$ is the matrix representation of estimated reflectance using the eigenvectors, represented in matrix \mathbf{E} , and the corresponding scalars, shown as matrix \mathbf{A} . The subscript E in $\hat{\mathbf{R}}_E$ indicates a result obtained using only eigenvectors without camera model or imaging.

After performing eigenvector analysis and checking the theoretical feasibility of the method, we introduced a camera model into the estimation as shown in Fig. 1. It was possible to simulate the digital camera's signals, represented by matrix \mathbf{D}_S , by Eq. (2).

$$\mathbf{D}_S = (\mathbf{S}\mathbf{F})^T \mathbf{P}\mathbf{R} \quad (2)$$

where the matrix \mathbf{S} is the measured camera spectral sensitivities, the matrix \mathbf{F} is the spectral transmittances of the filters, \mathbf{P} is a diagonal matrix with illumination spectral power distribution, \mathbf{D}_S is the matrix of simulated camera signals and T denotes matrix transpose. A transformation matrix \mathbf{M}_S^- was calculated to estimate the matrix of eigenvectors coefficients, \mathbf{A} , from simulated camera signals, \mathbf{D}_S , as shown in Eq. (3)

$$\mathbf{A} = \mathbf{M}_S^- \mathbf{D}_S \quad (3)$$

The superscript $-$ is used since the transformation is obtained by a generalized inverse matrix calculation. This superscript was employed in the notation of all matrices obtained by inverting matrices and models. The estimated spectral reflectances, represented in matrix $\hat{\mathbf{R}}_S$, were calculated from simulated digital signals \mathbf{D}_S using the eigenvectors, \mathbf{E} , as shown in Eq. (4).

$$\hat{\mathbf{R}}_S = \mathbf{E}\mathbf{M}_S^- \mathbf{D}_S \quad (4)$$

The performance of the estimation was evaluated comparing measured original target spectral reflectances, \mathbf{R} , with estimated spectral reflectances, $\hat{\mathbf{R}}_S$.

In digital camera-imaging system, it is also possible to linearly relate the camera signals, represented as matrix \mathbf{D} , to the estimated reflectances, shown as matrix $\hat{\mathbf{R}}_I$, by deriving a transformation matrix, \mathbf{M}_I^- , from camera signals, \mathbf{D} , to the matrix \mathbf{A} of scalars of the eigenvectors, \mathbf{E} , shown in Eq. (5).

$$\hat{\mathbf{R}}_I = \mathbf{E}\mathbf{M}_I^- \mathbf{D} \quad (5)$$

The subscript I in $\hat{\mathbf{R}}_I$ and \mathbf{M}_I^- indicates matrices related to imaging process using actual camera signals. The calculation of the transformation matrix, \mathbf{M}_I^- , has been a topic of research at MCSL.³⁵

The estimated reflectances, $\hat{\mathbf{R}}_I$, were then used to estimate the area coverages for CMYK inks using the transformation matrix, \mathbf{M}_P^- , that was obtained by inverting the printer model. We based our printer model on the Yule–Nielsen modified spectral Neugebauer equation³⁶ for four inks:

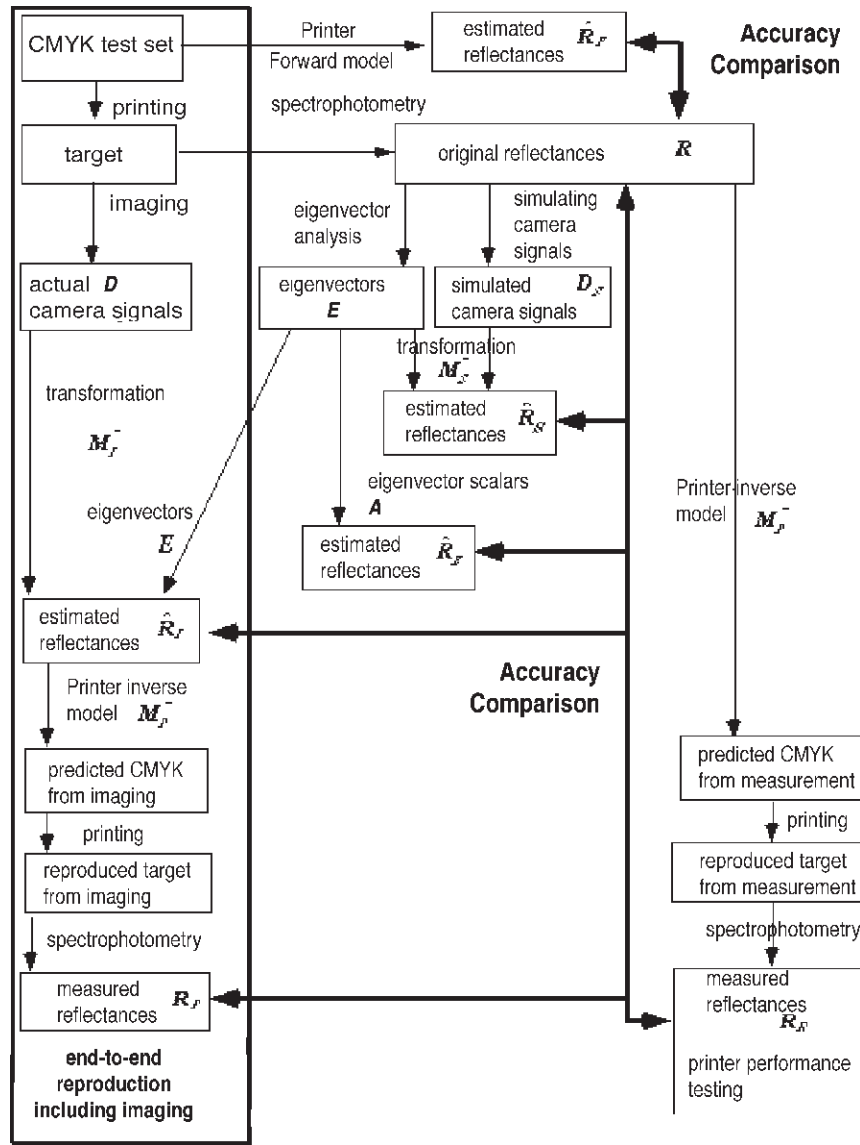


Figure 1. Block diagram of the spectral color reproduction system and its evaluation.

$$\hat{\mathbf{r}}_F = \left[\sum_{i=1}^{16} f_i \mathbf{r}_{i,\max}^{1/n} \right]^n \quad (6)$$

where the vector $\hat{\mathbf{r}}_F$ is the estimated printed spectral reflectance, n is the empirically fit Yule–Nielsen n -factor accounting for physical and optical dot gain, the vector $\mathbf{r}_{i,\max}$ is the spectral reflectance of the i^{th} Neugebauer primary, the scalar f_i is the Demichel weighting of the i^{th} Neugebauer primary defined by the product of the effective areas, w_j for each ink given by Eq. (7) using the nomenclature of Ref. 22:

$$f_i = \prod_{j=1}^4 \begin{cases} \text{if ink } j \text{ is in Neugebauer primary } i, \text{ then } w_j \\ \text{else, } (1 - w_j) \end{cases} \quad (7)$$

The matrix $\hat{\mathbf{R}}_p$ is composed by the vectors $\hat{\mathbf{r}}_F$ in its columns. The effective dot areas w_j are different from the corresponding theoretical dot areas sent to the

printer due to mechanical and optical dot gain. The transformation from theoretical to effective dot areas can be accomplished using an optimized mathematical approximation. A first order approximation can be achieved using high order polynomials or nonlinear interpolation. Further improvement can be achieved using models for ink and optical trapping. In this research, look-up tables were created using nonlinear interpolation. The subscript P in the matrices \mathbf{R}_p and \mathbf{M}_p^- corresponds to the printer processing using estimated spectral reflectances from actual camera signals. Since Eq. (6) is not analytically invertible, nonlinear optimization was used to calculate the transformation \mathbf{M}_p^- . Cascading these transformations, the end-to-end spectral color reproduction transformation from digital camera signals to printer area coverages is shown in Eq. (8).

$$\mathbf{M}_p^- \mathbf{E} \mathbf{M}_s^- \quad (8)$$

Experimental

In our experiments, we used a medium spatial resolution trichromatic IBM PRO/3000 digital camera system ($3,072 \times 4,096$ pixels, R, G, B filter wheel, dark current corrected 12 bits per channel that has a $45^\circ/0^\circ$ imaging configuration and tungsten illumination).³⁷ The spectral sensitivities of the IBM PRO/3000 digital camera system were measured, as well as the spectral radiant power of the image capture illuminant. White spatial correction was performed on the captured image to account for spatial non-uniformity of the illumination. For the printer, we used an Epson Photo Style™ 1200 ink jet printer; although it has six ink capability using light cyan and light magenta besides CMYK inks, only the CMYK inks were used. Given that a target such as the GretagMacbeth ColorChecker™ color rendition chart has many out-of-gamut colors,²⁴ a target was created using the ink jet printer, thus insuring all colors were in gamut. A special driver was used to assure control of the area coverages of each ink during the printing process. A target with 55 colors sampled along several hue axes was generated. An image of the target as well as the color distribution of the target in CIELAB space for illuminant D50 and the 2° observer is shown in **Color Plate 17, page 593**. All the spectral measurements were performed using a Gretag Spectrolino $45^\circ/0^\circ$ spectrophotometer. Five prints of the target image were measured. For each color, we calculated the mean color difference from the mean, MCDM.³⁸ The mean color difference from the mean, MCDM, is calculated as shown in Eq. (9) where each i^{th} L_i^* , a_i^* and b_i^* measurement is compared with its corresponding average, \bar{L}^* , \bar{a}^* , and \bar{b}^* , followed by summation of the N color differences, then dividing by the numbers of measurement, N .³⁸ Equation (9) shows a general concept that can be extended to different color difference equations.

$$MCDM = \frac{\sum_{i=1}^N \left[(L_i^* - \bar{L}^*)^2 + (a_i^* - \bar{a}^*)^2 + (b_i^* - \bar{b}^*)^2 \right]^{1/2}}{N} \quad (9)$$

The average MCDM for all 55 colors was $0.23 \Delta E_{94}^*$. The maximum MCDM was $1.1 \Delta E_{94}^*$. Considering that this result included measurement uncertainty, we concluded that the printer had sufficient accuracy. These values represent an upper limit of performance when modeling the printer.

It was necessary to consider both color accuracy from the visual point of view as well as the accuracy of spectral reflectance estimation. Since there is no consensus of which metric is the best for evaluating spectral matches,³⁹ we used two color difference equations, two metrics of spectral curve difference and a metameric index calculation based on the parametric decomposition proposed by Fairman.⁴⁰ The metameric index compares the extent to which two spectra are different between a reference condition and a test condition under different illuminants or observers. In particular, if we employ the metameric index using Fairman parametric decomposition, at first, we correct the test spectrum until an exact tristimulus equality is achieved under a reference condition. Then, the metameric index is calculated using a CIE color difference equation for a test illuminant and observer. Details of the calculation can be found in Refs. 38 and 40. For the color difference equation, we used CIEDE2000 since it incorporates the latest advances in color dif-

ference specifications. For the spectral curve difference metrics, we used the root mean square error (rms) between original and estimated spectra and the goodness-of-fit coefficient (GFC).⁴¹ GFC is based on the inequality of Schwartz having values between 0 and 1 and indicates the correlation between two spectral curves; a value of unity corresponds to a perfect spectral match. The metric is calculated using Eq. (10).

$$GFC = \frac{\left| \sum_j R_m(\lambda_j) R_e(\lambda_j) \right|}{\sqrt{\sum_j [R_m(\lambda_j)]^2} \sqrt{\sum_j [R_e(\lambda_j)]^2}} \quad (10)$$

where $R_m(\lambda_j)$ is the measured original spectral data at the wavelength λ_j and $R_e(\lambda_j)$ is the estimated spectral data at wavelength λ_j . $GFC \geq 0.999$ and $GFC \geq 0.9999$ are required for respectively good and excellent spectral matches.⁴¹

All colorimetric accuracy calculations in this article were computed using illuminant D50 and the 2° standard observer. For the metameric index calculation, D50 was used as the reference illuminant and illuminant A was used as the test illuminant. CIEDE2000 was also used in the metameric index calculation. In general, a CIEDE2000 of less than unity, a metameric index of less than unity, and rms error of less than 1% are good color matches. We also evaluated plots of the spectral difference between originals and their estimates as a function of wavelength. These plots were used to indicate spectral regions that have reduced performance.

Results and Discussions

The evaluation of the color accuracy of our spectral color-reproduction system was divided in three parts: spectral reflectance estimation accuracy of the MVSI acquisition system, spectral-based printing model accuracy, and end-to-end system accuracy.

Evaluation of the MVSI Acquisition System

The accuracy of the spectral estimation from the multi-channel acquisition can be evaluated starting from the analysis of the eigenvector reconstruction, adding simulated camera signals and concluding with spectral estimation from actual camera digital signals. That is, estimation uncertainty was added progressively.-

Performance of Eigenvectors in the Reconstruction of Original Spectra

Eigenvector analysis was evaluated theoretically by reconstructing the spectral reflectances, $\hat{\mathbf{R}}_E$, from the derived eigenvectors and scalars as shown in Fig. 1. The number of eigenvectors used to estimate the reflectances was selected comparing the estimated reflectances, $\hat{\mathbf{R}}_E$, with the measured spectral reflectances, \mathbf{R} , of the original target.

The spectral reflectances of the printed target with 55 colors were measured and eigenvector analysis performed. Table I shows the cumulative contribution for each multiple-of-three eigenvectors and the influence of the number of eigenvectors on the colorimetric and spectral accuracy of the spectral estimation. We only consider eigenvector triplets since we were using triplets of RGB digital signals from our camera without and with the use of one or more colored absorption filters.

TABLE I. Cumulative variance contribution and influence of the number of eigenvectors used in the spectral reconstruction of printed targets on its colorimetric and spectral accuracy. This table corresponds to Fig. 2.

Number of eigenvectors	Cumulative variance contribution (%)	Mean ΔE_{00} (D50, 2°)	Mean Spectral rms error (%)	Mean GFC (%)	Mean Metameric Index (ΔE_{00}) (D50 -> A, 2°)
3	98.10	5.1	2.7	97.53	1.4
6	99.97	0.4	0.8	99.77	0.2
9	99.99	0.1	0.4	99.95	0.03
12	100.00	0.1	0.2	99.98	0.01

The usual result was observed. As the number of eigenvectors increased, estimation accuracy improved. Selecting the number of eigenvectors was a balance between estimation accuracy and minimizing the number of image planes. For these samples, six eigenvectors were selected. The spectral differences between measured and estimated spectra are plotted in Fig. 2. Reconstructions using six eigenvectors resulted in maximum colorimetric error of less than $1 \Delta E_{00}$ and an average spectral reflectance rms error less than 1%. The GFC and metamerism index metrics were also good. From Table I, it is possible to see that six eigenvectors can reconstruct the original spectra with 99.97% accuracy. The effect of dimensionality reduction is shown in Fig. 2. The relatively large reflectance difference in the short-wavelength region was caused by the six eigenvectors poorly estimating the mean reflectance. Typical camera transformations do not include the mean reflectance. Had we selected more eigenvectors, the mean reflectance would have been well estimated; its omission would have been inconsequential. It is also worth noting that although only four inks were used, dimensionality reduction to four eigenvectors would result in poor spectral accuracy. This is kind of indirect evidence that the Yule-Nielsen n value is required to achieve linearity between the amount of ink on paper and spectral reflectance, shown in Eq. (6).

Estimation of Spectral Reflectance Using Simulated Camera Signals

The measured spectral properties of the IBM PRO/3000 digital camera system and a Kodak Wratten filter 38 (light blue) were used to simulate camera signals. This filter was chosen after an optimization process that resulted in a filter with transmission characteristics similar to light blue. Figure 3 shows the spectral sensitivities of the IBM digital camera with and without light blue filtering. The trichromatic system without filtering and with the light blue filter give six signals, used in conjunction with the six reflectance eigenvectors in order to estimate the spectral reflectance from simulated camera signals. This analysis using simulated camera signals was important because it tested the performance of the estimation system in the absence of imaging uncertainty such as noise. Table II shows the colorimetric and spectral accuracy between measured spectra and estimated spectra. Figure 4 shows the spectral difference between original and estimated spectra.

It is possible to see from Table II and Fig. 4 that the estimation of spectral reflectance from the six simulated digital signals and six eigenvectors produced reasonable colorimetric performance but had problems in the spectral predictions with large errors in the long-wavelength region of visible spectrum. The spectral error present in the theoretical evaluation using eigenvectors was amplified with the introduction of the imaging system. The introduction of the camera model resulted in

larger errors due to a lack of fit between scalars and simulated camera signals. In order to improve the performance we have to use a better transformation rather than the generalized pseudo-inverse. This is a current topic of research at MCSL.³⁵

Estimation of Spectral Reflectance Using Actual Camera Signals

As in the evaluation of the spectral estimation using simulated camera signals, the estimation of the spectral reflectance using actual camera signals also relies on *a priori* spectral analysis but instead of using simulated camera signals, D_s , it used camera signals, D , obtained by actual imaging. The performance of the estimation was evaluated comparing measured original target spectral reflectances, R , with estimated spectral reflectances, \hat{R}_l , from camera signals, D , using transformation M_l .

The trichromatic system without filtering and with the light blue filter produced six channel images. The camera signals of each color of the target were averaged. Then, the average camera signals for each color were used in conjunction with six eigenvectors of spectral reflectance to estimate spectral reflectance from camera digital signals. Table III shows the colorimetric and spectral performance. Figure 5 shows the absolute spectral difference between original and estimated spectra.

Comparing Tables II and III as well as the spectral differences of Figs. 4 and 5, we see that the performance was worse in the spectral reconstruction using actual camera signals than using simulated camera signals. This result was expected because of the introduction of noise, quantization, and typical experimental uncertainty when actual camera signals were used. In order to improve results, we have to consider better transformations that include noise aspects of imaging.⁴

Figure 6 shows a comparison of the spectral estimation of one of the target colors. The measurement of the original reflectance was compared with the reflectance estimated only by eigenvectors, the reflectance estimated by simulated camera signals, and the reflectance estimated by actual camera signals. The reflectance estimated using eigenvectors was almost a perfect match with the measured reflectance. Adding progressively more uncertainty to the estimation produced spectral curves that diverged progressively from the measured reflectance, as expected.

Evaluation of the Spectral-Based Printing System

The spectral-based printing system evaluation was subdivided in two different experiments. At first, we started with the evaluation of the spectral-based printing model predicting reflectance from color separations, and then we evaluated the spectral-based printing system predicting color separations from reflectance using as input, measured reflectances of the original target.

TABLE II. Colorimetric and spectral accuracy of reflectance estimation of the printed target using six eigenvectors and six simulated camera signals of the IBM PRO/3000 digital camera system. The simulated camera signals were obtained combining the trichromatic camera without and with a light blue filter. This table corresponds to Fig. 4.

Number of eigenvectors	ΔE_{00} (D50, 2°)	Spectral rms error (%)	GFC (%)	Metameric Index (ΔE_{00}) (D50 -> A, 2°)
Average	0.3	1.0	99.64	0.1
Maximum or Minimum (GFC)	0.8	2.9	98.70	0.5
Standard deviation	0.2	0.3	0.34	0.1

TABLE III. Colorimetric and spectral error of the reflectance estimation of the printed target using six eigenvectors and six actual camera signals for IBM PRO/3000 digital camera system. The camera signals were obtained combining the trichromatic camera without and with a light blue filter. This table corresponds to Fig. 5.

Number of eigenvectors	ΔE_{00} (D50, 2°)	Spectral rms error (%)	GFC (%)	Metameric Index (ΔE_{00}) (D50 -> A, 2°)
Average	1.0	1.4	99.55	0.4
Maximum or Minimum (GFC)	2.1	2.6	97.91	1.2
Standard deviation	0.4	0.4	0.40	0.3

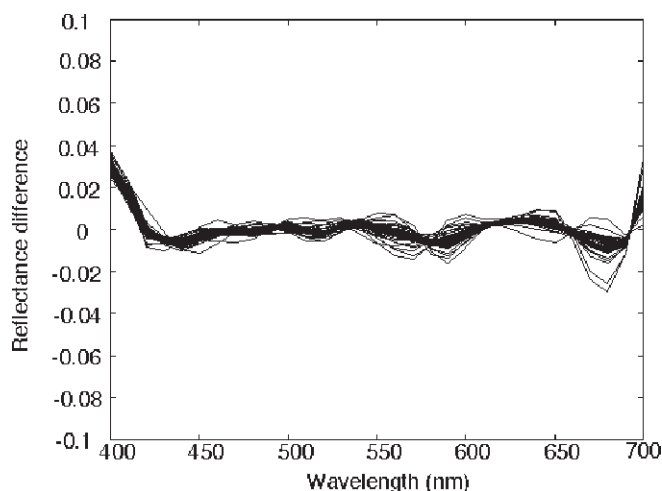


Figure 2. Spectral difference between measured spectral reflectance, R , and estimated spectral reflectance, \hat{R}_E , using six eigenvectors.

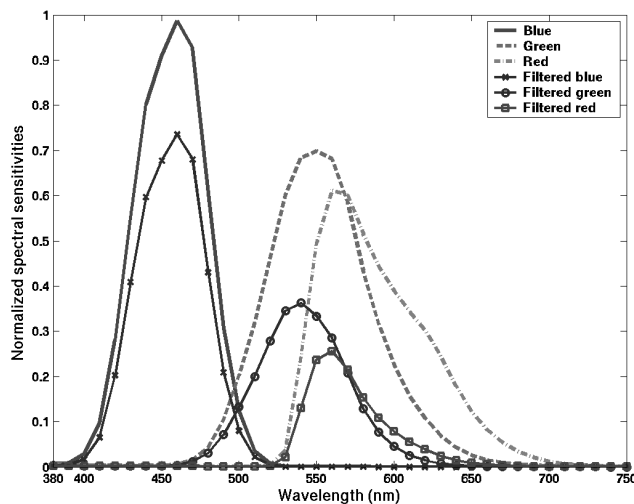


Figure 3. Spectral sensitivities of the IBM digital camera system with and without light blue filtering.

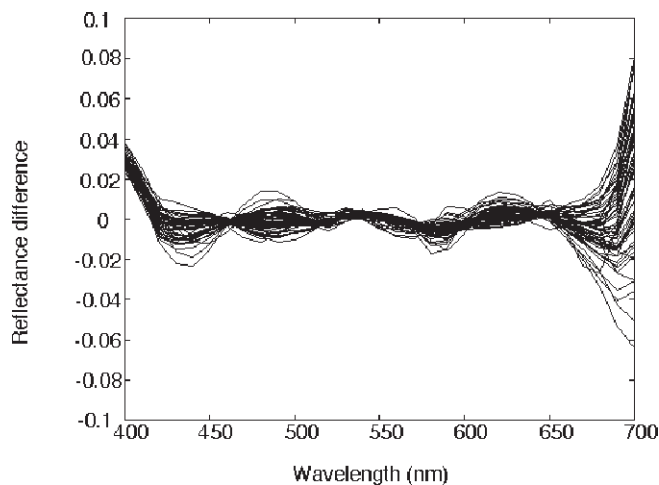


Figure 4. Spectral difference between measured spectral reflectances, R , and estimated spectral reflectances, \hat{R}_S , using six simulated digital camera signals, D_s , and six eigenvectors combined with transformation M_S^- .

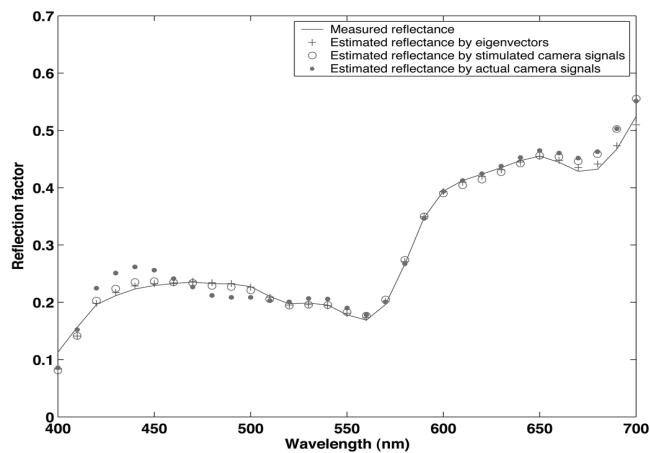


Figure 5. Spectral difference between measured spectral reflectances, R , and estimated spectral reflectances \hat{R}_I , from actual camera signals, D , using transformation M_I^- .

TABLE IV. Colorimetric and spectral evaluation of the model used in the spectral-based printing. This table corresponds to Fig. 7.

Number of eigenvectors	ΔE_{00} (D50, 2°)	Spectral rms error (%)	GFC (%)	Metameric Index (ΔE_{00}) (D50 -> A, 2°)
Average	0.3	0.1	99.996	0.05
Maximum or Minimum (GFC)	0.7	0.4	99.98	0.3
Standard deviation	0.1	0.1	0.004	0.1

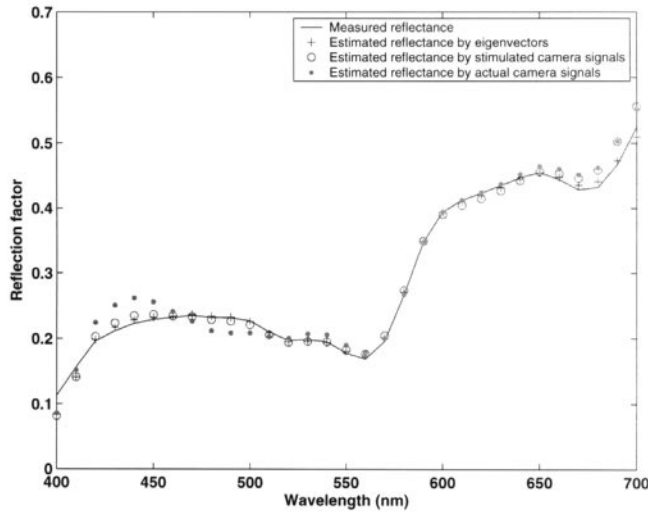


Figure 6. Comparison of spectral reflectance curves between the original (measured) and the estimations using only eigenvectors, using eigenvectors in conjunction with simulated camera signals, and using eigenvectors in conjunction with actual camera signals.

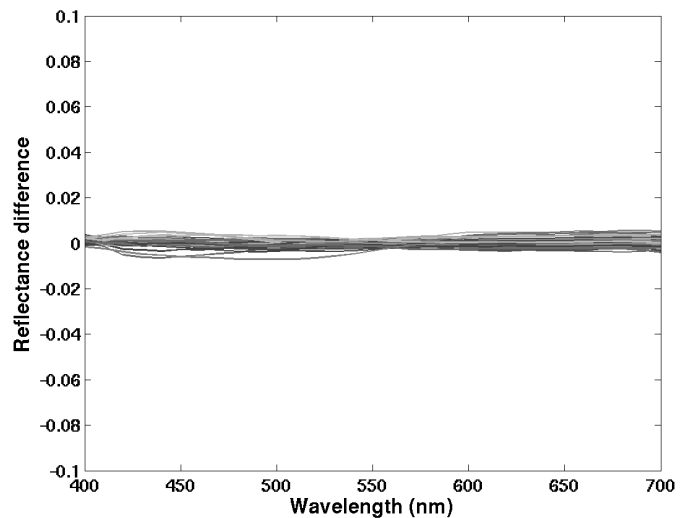


Figure 7. Comparison of spectral reflectance curves between the original (measured) and the estimations using only eigenvectors, using eigenvectors in conjunction with simulated camera signals, and using eigenvectors in conjunction with actual camera signals.

Evaluation of the Spectral-Based Printing Model

In the first analysis, diagrammed in the top of Fig. 1, we evaluated the accuracy of the Yule–Nielsen spectral Neugebauer Model to estimate spectral reflectance, $\hat{\mathbf{R}}_F$, from four color separations.

Ramps of each ink were printed in 17 equal steps in theoretical dot areas. In addition, the two, three, and four ink overprints at 100% theoretical dot area were also printed. These samples and the paper were measured. The determination of the Yule–Nielsen n -factor was carried out by stepping through all values of n -factor with increments of 0.1 from 1 to 20 and calculating the estimated reflectance and comparing with measured reflectances of the four primary ramps. For each sample, dot area was estimated minimizing RMS spectral error. See Refs. 30 and 31 for greater detail. These dot areas are referred as “effective dot areas.”⁴² An optimal n value was the one corresponding to the smallest average ΔE_{94}^* for all the colors of the primary ramps. The optimal n -factor was 2.9. The theoretical to effective dot area transfer functions were calculated for each primary ramp by discretely sampling at the effective dot area forming continuous transfer functions using cubic spline interpolation.

The performance of this printing model was tested using the target with 55 colors as an independent verification target. Figure 7 shows the spectral difference between original and estimated spectra. Table IV shows the colorimetric and spectral performance of the printing model. The printer model had excellent performance. All the results were within 1 ΔE_{00} and within GFC of 99.98%. For this particular printer, inks, and paper, it was not necessary to consider more complex models, summarized in Ref. 42.

Evaluation of the Spectral-Based Printing System

In the second experiment, shown in the right side of the Fig. 1 flowchart, we evaluated the accuracy of the spectral-based printing system. The measured spectral reflectances of the target, \mathbf{R} , were used in conjunction with the printer inverse model, \mathbf{M}_P^{-1} to predict the CMYK color separations. Then, the target was reproduced by directly sending the CMYK dot areas to the printer. The spectral reflectances, represented by matrix \mathbf{R}_R , of the printed targets were measured. The evaluation of the printing system without introducing uncertainty from the spectral estimation using the camera was performed comparing the measured spectral reflectances, \mathbf{R} , of the original printed target with the measured spectral reflectances, \mathbf{R}_R , of the reproduced target.

The printer inverse model, \mathbf{M}_P^{-1} , was implemented using the Matlab 5.3 *fmincon* optimization tool. There was a convergence problem for one color and it was excluded from the analysis of the results, shown in Table V and Fig. 8. We believe that the convergence problem for a particular dark color was due to the initial value that was 50% for all area coverages. From these results, we concluded that the spectral-based printing system had reasonable accuracy. The spectral printing system performance was worse than the spectral printing model. This was expected, because it included actual printing and its associated uncertainties.

Evaluation of the Spectral Color Reproduction System from Original to Hardcopy

Finally, the end-to-end spectral reproduction system was evaluated. In this case, the spectral reflectances used to predict CMYK area coverages were the esti-

TABLE V. Colorimetric and spectral evaluation of the spectral-based printing system. The evaluation of the spectral-based printing is a comparison between measured original target and measured reproduced target obtained by printing the target estimated using measured reflectances of the original target. This table corresponds to Fig. 8.

Number of eigenvectors	ΔE_{00} (D50, 2°)	Spectral rms error (%)	GFC (%)	Metameric Index (ΔE_{00}) (D50 -> A, 2°)
Average	0.9	0.7	99.91	0.1
Maximum or Minimum (GFC)	4	2	99.57	0.4
Standard deviation	1	0.5	0.07	0.1

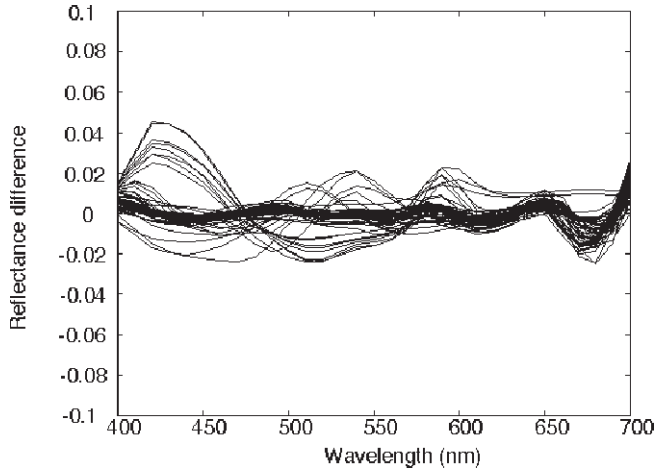


Figure 8. Spectral difference between measured original target reflectances, \mathbf{R} , and measured reproduced target reflectances, $\hat{\mathbf{R}}_p$, after using printer inverse model and printing the target.

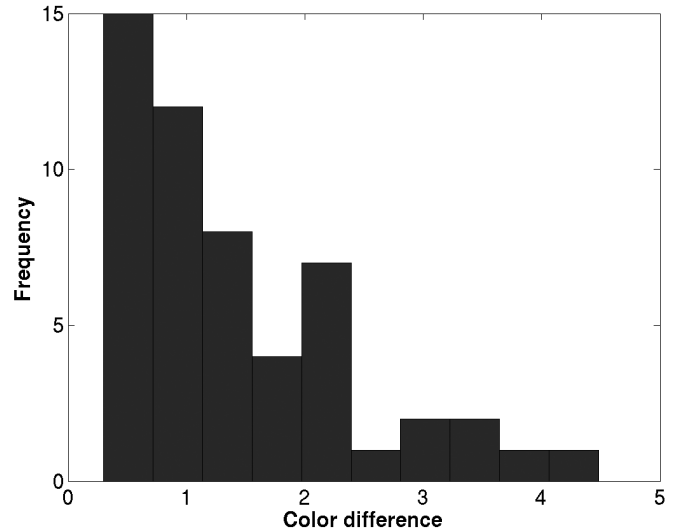


Figure 9. ΔE_{00} histogram between the originally measured spectral reflectances and the measured reflectances of the reproduced target. It corresponds to the evaluation of the entire system from end-to-end including imaging and printing represented in the diagram of Fig. 1.

mated spectral reflectances, represented by matrix $\hat{\mathbf{R}}_t$, obtained from actual camera signals, \mathbf{D} . That is, the CMYK area coverages were obtained applying the transformation $\mathbf{M}_p \mathbf{E} \mathbf{M}_t^{-1}$ to the actual camera signals, \mathbf{D} . A print was made and its reflectances, \mathbf{R}_p , measured. The measured reflectances, \mathbf{R} , of the original target were then compared to the measured reflectances, \mathbf{R}_p , from the hardcopy. This evaluated the end-to-end spectral color reproduction system performance.

Table VI summarizes the colorimetric and spectral accuracy. Figure 9 shows the histogram of ΔE_{00} between measured spectral reflectances of the original target and its end-to-end reproduction. Figure 10 shows the spectral difference. From the results in Table VI and Figs. 9 and 10, the end-to-end spectral-based color reproduction system had reasonable accuracy and demonstrated the feasibility of the proposed spectral color reproduction system. Figure 11 shows the comparison between the measured spectral reflectance of a sample in the original target and its corresponding measured spectral reflectance after applying the printer inverse model to it followed by printing; and its corresponding measured spectral when the camera imaging was introduced. From Fig. 11, it is possible to see that the spectral curve diverged progressively from the measured spectral reflectance of the original target as we added first the printing model and then the digital camera imaging. Figure 12 shows three examples each of the best and worst spectral matches using the criteria of colorimetric, GFC error and metameric index metrics.

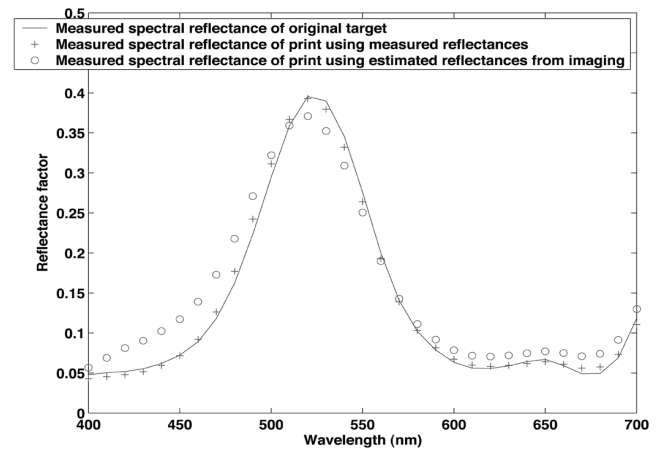


Figure 10. Spectral difference between the originally measured spectral reflectances, \mathbf{R} , and the measured reflectances, $\hat{\mathbf{R}}_p$, of the reproduced target. It corresponds to the evaluation of the entire system from end-to-end including imaging and printing represented in the diagram of Fig. 1.

TABLE VI. End-to-end system colorimetric and spectral evaluation between original target and printed target. The original target was imaged using six channels of IBM PRO/3000 actual camera signals (obtained combined the trichromatic signal without filtering and with light blue Kodak Wratten absorption filter). Six eigenvectors from the target were used in the spectral estimation. The estimated reflectances were then converted to CMYK area coverages using the printer inverse model and finally the target was reproduced using Epson Photo Stylus 1200. This table corresponds to Figs. 9 and 10.

Number of eigenvectors	ΔE_{00} (D50, 2°)	Spectral rms error (%)	GFC (%)	Metameric Index (ΔE_{00}) (D50 → A, 2°)
Average	1.5	0.9	99.79	0.2
Maximum or Minimum (GFC)	5.5	2.8	98.67	0.6
Standard deviation	1.1	0.5	0.28	0.1

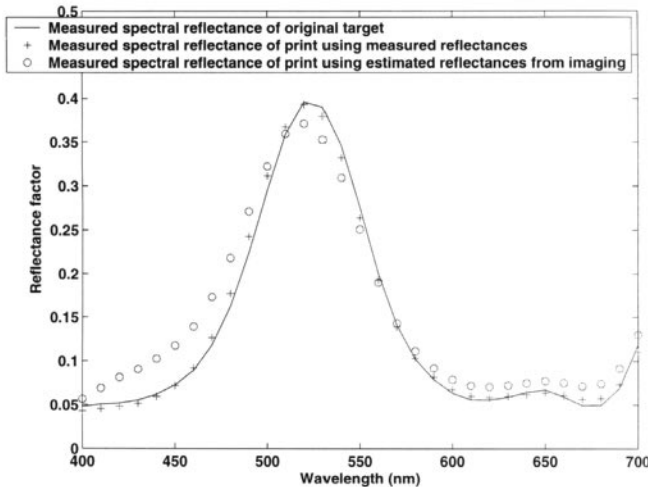


Figure 11. Comparison of spectral reflectance curve of one color sample of the target obtained by measuring the spectral reflectance of the original target, the spectral reflectance of the hardcopy obtained by applying the spectral-based printer to the measured original target, and finally reflectance of the hardcopy obtained by applying the spectral-based printer to reflectances estimated by the imaging system (end-to-end system evaluation).

Conclusions

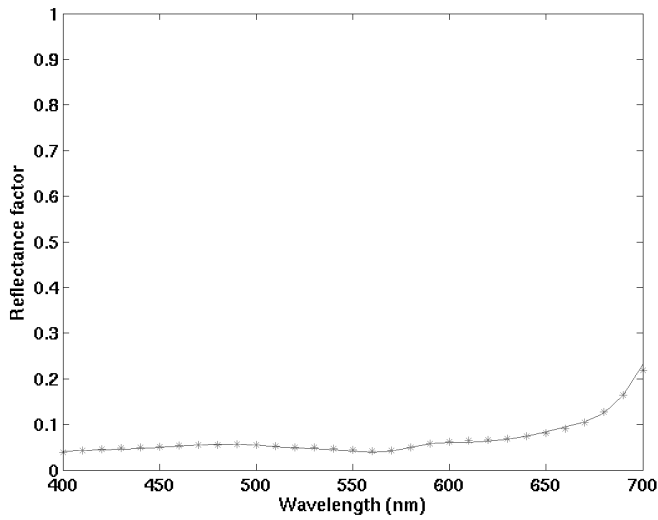
This research is part of our effort to integrate spectral image capture with multi-ink printing. An end-to-end spectral color reproduction system was tested with printer in-gamut colors. The performance was evaluated in terms of colorimetric accuracy, spectral reflectance difference metrics, and a metameric index. In the image acquisition side, the performance of the wide band acquisition system was verified by imaging a printed ink target. The experiments were performed in three steps: spectral analysis, spectral reconstruction using simulated camera signals and spectral reconstruction using actual camera signals. The spectral analysis indicated the theoretical feasibility of using six eigenvectors to reconstruct reflectance spectra. The spectral reconstruction using simulated camera signals allows the analyses of the results without typical imaging noise. The spectral estimation based on the actual camera signals presented an average colorimetric accuracy of 1.0 ΔE_{00} and spectral reflectance rms error of 1.4% when the measured spectral reflectances of the printed targets were compared to the estimated spectral reflectances using the digital camera system.

The printing system also was evaluated progressively, first estimating the accuracy of the spectral printing model using only simulated spectral reflectances generated by the printer spectral-based model and then evaluating the spectral-based printing system accuracy that included the inverse-model. The spectral-based printing had remarkably good performance. The spectral printing system had an average colorimetric accuracy 0.9 ΔE_{00} and spectral reflectance rms error of 0.7%. This result excluded one color that had convergence problems during model inversion. We believe that the convergence problem for a particular dark color patch was due to the initial value that was 50% for all area coverages.

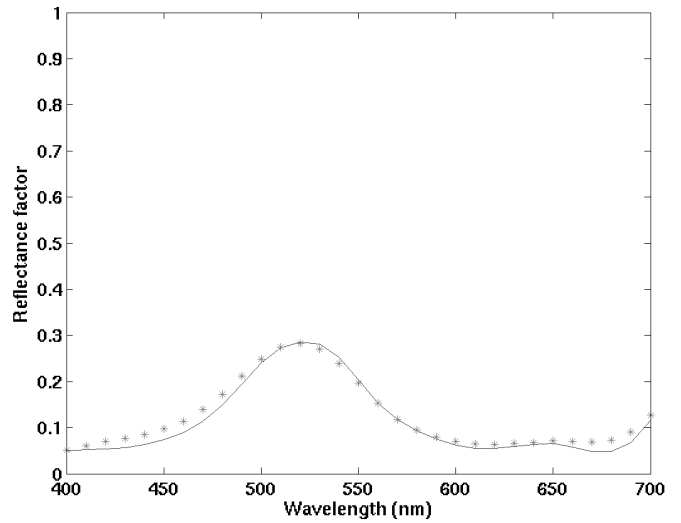
Finally, the entire end-to-end spectral reproduction system had an average colorimetric accuracy of 1.5 ΔE_{00} and spectral reflectance rms error of 0.9%.

This research also was able to show how error is added progressively in the image acquisition and reproduction system from theoretical modeling, to system simulation, to actual imaging. These results showed the feasibility to image and reproduce in-gamut colors using a CMYK ink jet printing system. Conventional four color printing systems are limited in terms of degrees of freedom in representing the properties of spectral information. Therefore there are limitations in trying to minimize metamerism using four color printing. The existing multiple ink hardcopy systems that use more than four inks (whose primary focus is expanding the color gamut) do not address the problem of metamerism since their color separation algorithms are colorimetric and not spectral in nature. If the printer has a large set of inks from which to choose from, it should be possible to select a subset of inks that achieve a spectral match between original objects and their printed reproductions by spectral reflectance image estimation, ink selection minimizing metamerism,²⁷ and spectral-based printing models including separation algorithms.^{22,23,29,32,34} Different printing modeling approaches also can be considered.³⁶ It is also necessary to address improvements in the input end of the system, providing better transformations from digital signals to reflectance spectra.³⁵

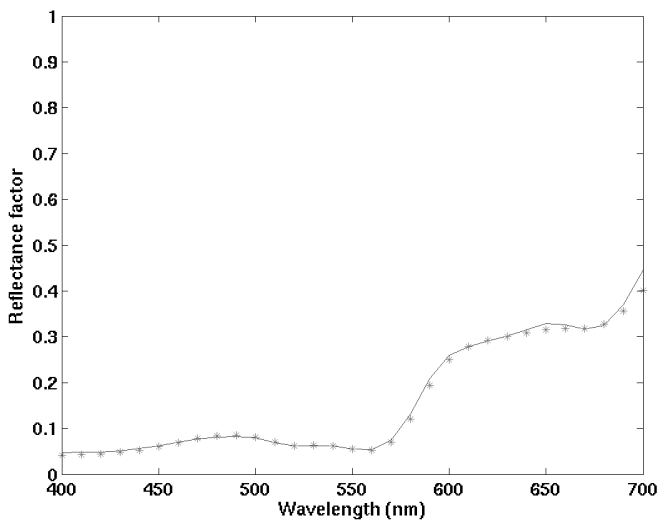
The spectral matching capabilities of the spectral-based printing system would require far more computational power than that needed for the traditional metameric approach. We also have to address efficient approaches to processing images where tradeoffs can be considered between desired precision, processing time requirements, and available computational power and memory constraints.²³ Efficiency could be achieved by reducing the dimensionality demands of spectral color management,³³ or building low dimensional lookup tables. Without such approaches, spectral color management would remain a very slow process or would make memory demands far exceeding current capabilities. ▲



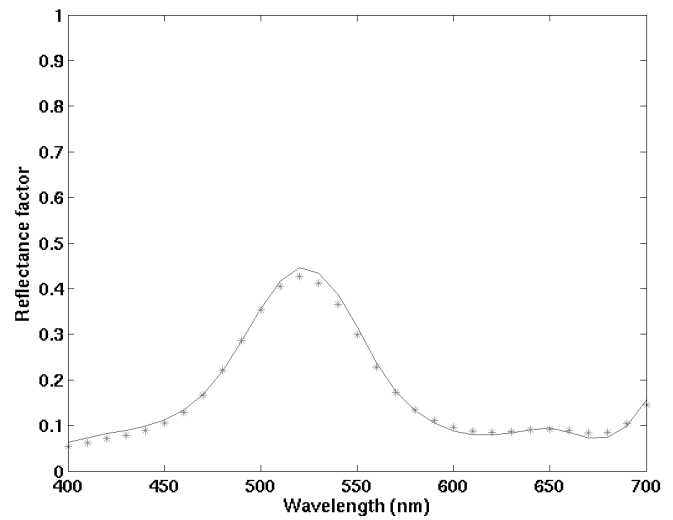
(a) Best match according to ΔE_{00}



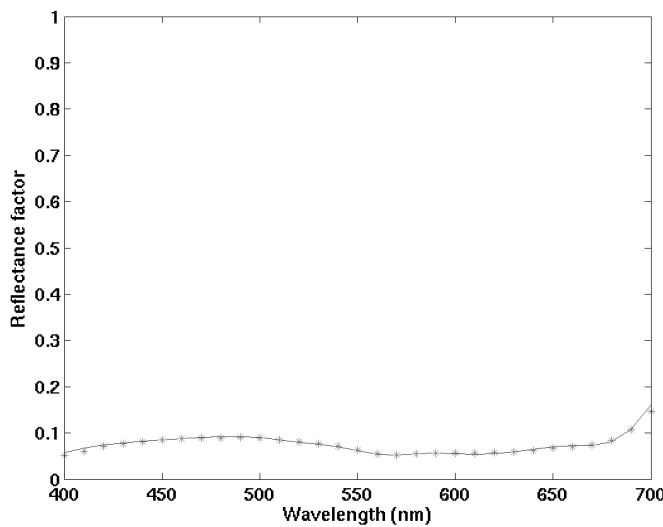
(b) Worst match according to ΔE_{00}



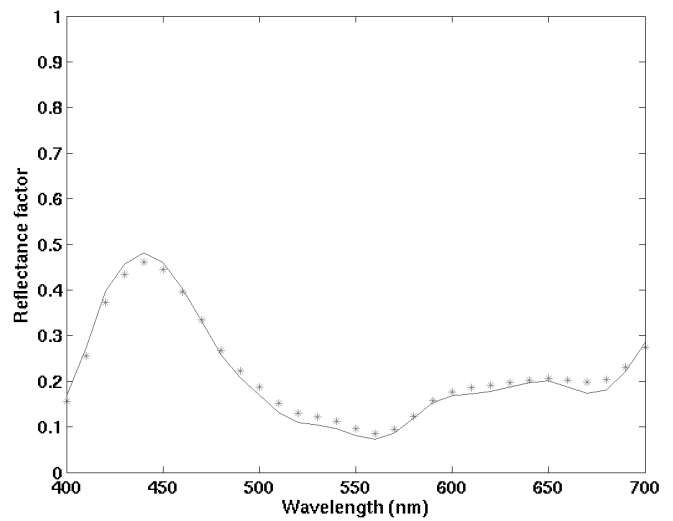
(c) Best match according to GFC metric



(d) Worst match according to GFC metric



(e) Best match according to metameric index



(f) Worst match according to metameric index

Figure 12. Examples of spectral matches between original target (solid line) and reproduced target using the spectral-based end-to-end reproduction system (stars).

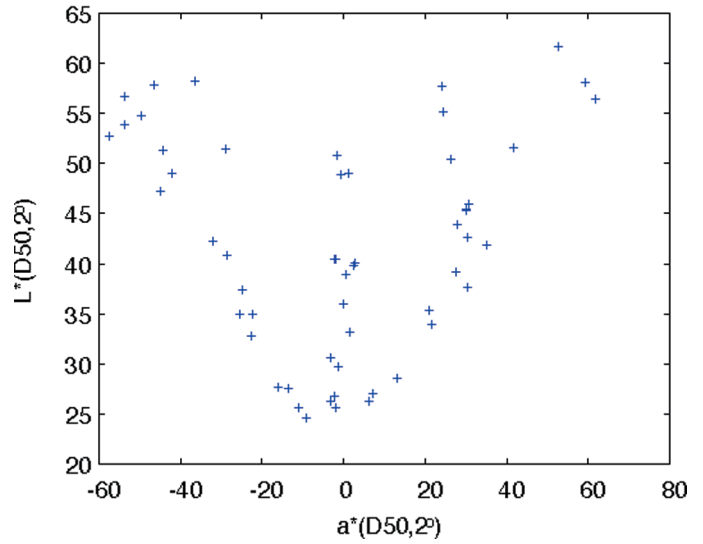
Acknowledgment. The authors would like to express their gratitude to E. I. du Pont de Nemours and Company, Inc. for their support of this research. We would also like to acknowledge the work of many members of the Munsell Color Science Laboratory who are working on building end-to-end spectral-based systems, especially Mitchell Rosen and Lawrence Taplin.

References

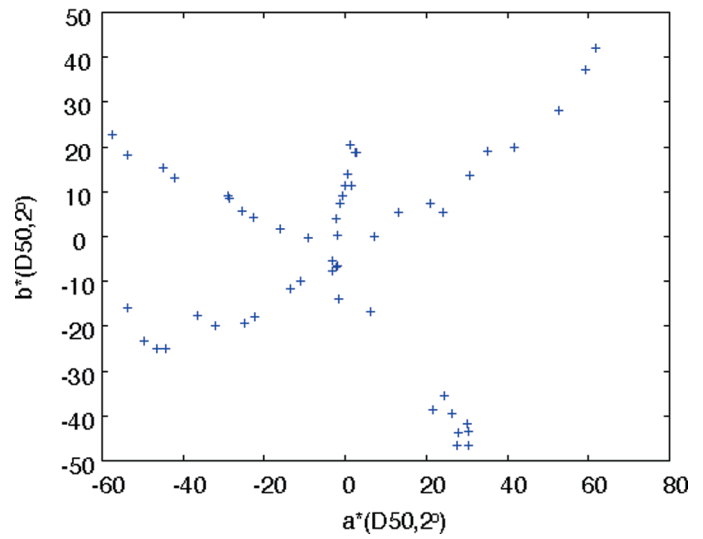
1. J. Cupitt, K. Martinez and D. Saunders, A methodology for art reproduction in colour: the Marc project, *Computers and the History of Art* **6**, 1–19 (1996).
2. R. S. Berns and D. M. Reiman, Color managing the third edition of Billmeyer and Saltzman's Principle of Color Technology, *Color Res. Appl.* **27**, 360–373 (2002).
3. B. Hill, (R)evolution of color imaging systems, in *Proc. First European Conference on Color in Graphics, CGIV'2002, Imaging and Vision*, IS&T, Springfield, VA, 2002, pp. 473–479.
4. H. Haneishi, T. Hasegawa, A. Hosoi, Y. Yokoyama, N. Tsumura, and Y. Miyake, System design for accurately estimating the spectral reflectance of art paintings, *Appl. Opt.* **39**, 6621–6632 (2000).
5. R. S. Berns, F. H. Imai, P. D. Burns, and D. Tzeng, Multispectral-based color reproduction research at the Munsell Color Science Laboratory, in *Electronic Imaging: Processing, Printing and Publishing in Color*, *Proc. SPIE* **3409**, 14–25 (1998).
6. F. Schmitt, H. Brettel and J. Y. Hardeberg, Multispectral Imaging Development at ENST, in *Proc. First International Symposium on Multispectral Imaging and High Accuracy Color Reproduction*, Chiba University, Chiba, Japan, 1999, pp. 58–64.
7. P. D. Burns and R. S. Berns, Analysis of multispectral image capture, in *Proc. 4th IS&T/SID Color Imaging Conference*, IS&T, Springfield, VA, 1996, pp. 19–22.
8. F. König and W. Præfke, The practice of multispectral image acquisition, *Proc. SPIE* **3409**, 34–41 (1998).
9. S. Tominaga, Spectral Imaging by a Multi-Channel Camera, in *Proc. SPIE* **3648**, 38–47 (1999).
10. M. Rosen and X. Jiang, Lippmann2000: A spectral image database under construction, in *Proc. International Symposium on Multispectral Imaging and Color Reproduction for Digital Archives*, Chiba University, Chiba, Japan, 1999, pp. 117–122.
11. S. Toyooka, K. Miyazawa and M. Hauta-Kasari, Low-dimensional multispectral image analyzing system with optimized broad band filters, in *Proc. Second International Symposium on Multispectral Imaging and High Accuracy Color Reproduction*, Chiba University, Chiba, Japan, 2000, pp. 59–66.
12. F. H. Imai and R. S. Berns, Spectral Estimation Using Trichromatic Digital Cameras, in *Proc. International Symposium on Multispectral Imaging and Color Reproduction for Digital Archives*, Chiba University, Chiba, Japan, 1999, pp. 42–49.
13. F. H. Imai, R. S. Berns and D. Tzeng, A comparative analysis of spectral reflectance estimated in various spaces using a trichromatic camera system, *J. Imaging Sci. Technol.* **44**, 280–287 (2000).
14. F. H. Imai, M. R. Rosen and R. S. Berns, Comparison of spectrally narrow-band capture versus wide band with a priori sample analysis for spectral reflectance estimation, in *Proc. IS&T/SID Eighth Color Imaging Conference*, IS&T, Springfield, VA, 2000, pp. 234–241.
15. F. H. Imai, S. Quan, M. R. Rosen and R. S. Berns, Digital camera filter design for colorimetric and spectral accuracy, in *Proc. Third International Conference on Multispectral Color Science*, University of Joensuu, Finland, 2001, pp. 13–16.
16. Y. Murakami, T. Obi, M. Yamaguchi, N. Ohshima and Y. Komiya, Spectral reflectance estimation from multi-band image using color chart, *Opt. Commun.* **188**, 47–57 (2001).
17. L. T. Maloney, Evaluation of linear models of surface spectral reflectance with small numbers of parameters, *J. Opt. Soc. Amer. A* **10**, 1673–1683 (1986).
18. T. Jaaskelainen, J. Parkkinen and S. Toyooka, Vector-subspace model for color representation, *J. Opt. Soc. Amer. A* **7**, 725–730 (1990).
19. M. J. Vrhel and H. J. Trussel, Color correction using principal components, *Color Res. Appl.* **17**, 328–338 (1992).
20. M. J. Vrhel, R. Gershon and L. S. Iwan, Measurement and analysis of object reflectance spectra, *Color Res. Appl.* **19**, 4–9 (1994).
21. D. H. Marimont and B. A. Wandell, Linear models of surface and illuminant spectra, *J. Opt. Soc. Amer. A* **9**, 1905–1913 (1990).
22. L. A. Taplin and R. S. Berns, Spectral color reproduction based on a six color inkjet output system, in *Proc. Ninth Color Imaging Conference*, IS&T, Springfield, VA, 2001, pp. 209–213.
23. M. R. Rosen, F. H. Imai, X. Jiang, and N. Ohta, Spectral reproduction from scene to hardcopy II: Image processing, *Proc. SPIE* **4300**, 33–41 (2001).
24. D. Tzeng, *Spectral-Based Color Separation Algorithm Development for Multiple-Ink Color Reproduction*, Ph. D. Thesis, RIT, Rochester, N.Y., 1999.
25. M. Kouzaki, T. Itoh, T. Kawaguchi, N. Tsumura, H. Haneishi, and Y. Miyake, Spectral Color Reproduction for Hardcopy System by using Vector Error Diffusion Method, in *Proc. First International Symposium on Multispectral Imaging and High Accuracy Color Reproduction*, Chiba University, Chiba, Japan, 1999, pp. 106–109.
26. D. Tzeng and R. S. Berns, Spectral-based ink selection for multiple-ink printing I. Colorant Estimation of Original Objects, in *Proc. Sixth IS&T/SID Color Imaging Conference*, IS&T, Springfield, VA, 1998, pp. 106–111.
27. D. Tzeng and R. S. Berns, Spectral-based ink selection for multiple-ink printing II. Optimal Ink Selection, in *Proc. Seventh IS&T/SID Color Imaging Conference*, IS&T, Springfield, VA, 1999, pp. 182–187.
28. D. Tzeng and R. S. Berns, Spectral reflectance prediction of ink overprints by Kubelka-Munk turbid media theory, in *Proc. TAGA/ISCC Symposium*, TAGA, Vancouver B.C., 1999, pp. 682–697.
29. D. Tzeng and R. S. Berns, Spectral-based Six color Separation minimizing Metamerism, in *Proc. Eighth IS&T/SID Color Imaging Conference*, IS&T, Springfield, VA, 2000, pp. 342–347.
30. K. Iino and R. Berns, Building Color Management Modules Using Linear Optimization I. Desktop color system, *J. Imaging Sci. Technol.* **42**, 79–94 (1998).
31. K. Iino and R. Berns, Building Color Management Modules Using Linear Optimization II. Prepress System for Offset Printing, *J. Imaging Sci. Technol.* **42**, 99–144 (1998).
32. F. H. Imai, M. R. Rosen, D. Wyble, R. S. Berns and D. Tzeng, Spectral reproduction from scene to hardcopy I: Input and Output, *Proc. SPIE* **4306**, 346–357 (2001).
33. M. Rosen, M. Fairchild, G. Johnson, and D. Wyble, Color Management within a Spectral Image Visualization Tool, in *Proc. Eighth IS&T/SID Color Imaging Conference*, IS&T, Springfield, VA, 2000, pp. 75–80.
34. L. A. Taplin, *Spectral modeling of a six color inkjet printer*, M. Sc. Thesis, Rochester Institute of Technology, 2001.
35. F. H. Imai, L. A. Taplin and E. A. Day, *Comparison of the accuracy of various transformations from multi-band images to reflectance spectra*, Munsell Color Science Laboratory Technical Report, RIT, Rochester, NY, 2002, <http://www.art-si.org/>
36. J. A. S. Viggiano, The color of halftone tints, *Proc. TAGA*, 647–661 (1985).
37. F. P. Giordano, G. W. Braudaway, J. Christensen, J. Lee, and F. Mintzer, Evolution of a High quality Digital Imaging System, *Proc. SPIE* **3650**, 110–118 (1999).
38. R. Berns, *Billmeyer and Saltzman's Principles of Color Technology*, 3rd ed., John Wiley and Sons, New York, 2000.
39. F. H. Imai, M. R. Rosen and R. S. Berns, Comparative study of metrics for spectral match quality, in *Proc. First European Conference on Color in Graphics, CGIV'2002, Imaging and Vision*, IS&T, Springfield, VA, 2002, pp. 492–496.
40. H. S. Fairman, Metameric correction using parametric decomposition, *Color Res. Appl.* **12**, 261–265 (1997).
41. J. Hernández-Andrés, J. Romero, J. L. Nieves and R. L. Lee Jr., Color and spectral analysis of daylight in southern Europe, *J. Opt. Soc. Amer. A* **18**, 1325–1335 (2001).
42. D. R. Wyble and R. S. Berns, A critical review of spectral models applied to binary color printing, *Color Res. Appl.* **25**, 5–19 (2000).



(a) Target image



(b) $a^* \times L^*$



(c) $a^* \times b^*$

Color Plate 17. Colorimetric plots for the target with 55 patches (D50 illuminant, 2° observer). (*Imai, et al.*, pp. 543–553)